Efficient Visible-to-UV Photon Upconversion Systems Based on CdS Nanocrystals Modified with Triplet Energy Mediators

ADVANCED FUNCTIONAL MATERIALS
www.afm-journal.de

Efficient Visible-to-UV Photon Upconversion Systems Based on CdS Nanocrystals Modified with Triplet Energy Mediators

*Lili Hou, Axel Olesund, Shameel Thurakkal, Xiaoyan Zhang, and Bo Albinsson**

Developing high-performance visible-to-UV photon upconversion systems based on triplet–triplet annihilation photon upconversion (TTA-UC) is highly desired, as it provides a potential approach for UV light-induced photosynthesis and photocatalysis. However, the quantum yield and spectral range of visible-to-UV TTA-UC based on nanocrystals (NCs) are still far from satisfactory. Here, three different sized CdS NCs are systematically investigated with triplet energy transfer to four mediators and four annihilators, thus substantially expanding the available materials for visible-to-UV TTA-UC. By improving the quality of CdS NCs, introducing the mediator via a direct mixing fashion, and matching the energy levels, a high TTA-UC quantum yield of 10.4% (out of a 50% maximum) is achieved in one case, which represents a record performance in TTA-UC based on NCs without doping. In another case, TTA-UC photons approaching 4 eV are observed, which is on par with the highest energies observed in optimized organic systems. Importantly, the in-depth investigation reveals that the direct mixing approach to introduce the mediator is a key factor that leads to close to unity efficiencies of triplet energy transfer, which ultimately governs the performance of NC-based TTA-UC systems. These findings provide guidelines for the design of high-performance TTA-UC systems toward solar energy harvesting.

1. Introduction

Ultraviolet (UV) light is responsible for many photochemical reactions,[1] including photocycloaddition, polymerization, photosynthesis, and photoisomerization, which play important roles in several natural processes, such as the formation of vitamin D for bone-strengthening.[2] Photocatalysis using UV light irradiation of wide-bandgap semiconductors has also an enormous potential for water splitting, in which the photon energy is converted into hydrogen, providing clean energy used in, e.g., fuel cells.[3] However, UV light from the sun is strongly attenuated by Earth's atmosphere. Triplet–triplet annihilation photon upconversion (TTA-UC),[4] a process in which low energy photons are readily converted to high energy photons under terrestrial solar irradiance conditions, is an emerging approach to produce UV light.[5]

In a TTA-UC system a triplet sensitizer and a triplet annihilator/emitter are needed to achieve upconversion. Photosensitizers generate their triplets by absorption of low energy photons and subsequent efficient intersystem crossing (ISC). The triplet energy of sensitizers then transfers to annihilators via triplet energy transfer (TET). Two triplet excited annihilators encounter and produce one singlet excited state that emits a high energy photon. So far, organic triplet sensitizers that have been applied to visible-to-UV TTA-UC are limited to biacetyl,[5a] Ir(III) complexes,[5e–g] and carbazolyl dicyanobenzene (CDCB) derivatives,[6] which feature several drawbacks such as large singlet-triplet gaps, low light absorptivity, and complicated synthesis to modify the triplet state energies. Alternatively, semiconductor nanocrystals (NCs), featuring high absorption cross sections as well as high and stable photoluminescence (PL) quantum yields, are attractive since they allow easy tuning of their optical bandgap through synthesis control of their shape and size.[7] Importantly, NCs have the capability to sensitize molecular triplets rapidly and efficiently, which represents a key step in the development of efficient TTA-UC systems.[8] This is typically achieved through binding of an organic ligand molecule, herein called the mediator, to the NC surface, which acts as a relay for TET between NC and annihilator.

Recent progress in the design of NC-based TTA-UC systems has enabled high upconversion quantum yields in the visible-to-visible region by pairing the NCs with the well-known blue-emitting annihilator diphenylanthracene (DPA). Ronchi et al. demonstrated that CdSe NCs doped with gold can achieve a TTA-UC quantum yield as high as 12% (out of a 50% maximum);[9a] CdSe NCs with an anthracene dihydrogen phosphate (ADP) ligand show a TTA-UC quantum yield of 8.5%;[9b] and $CuInS_2$ NCs with efficient energy transfer to the surface-anchored anthracene afford a TTA-UC quantum yield of 9.3%.[9c] However, the efficiencies for upconversion into the UV light region based on NCs and the spectral range of visible-to-UV TTA-UC based

L. Hou, A. Olesund, S. Thurakkal, X. Zhang, B. Albinsson
Department of Chemistry and Chemical Engineering
Chalmers University of Technology
Gothenburg 412 96, Sweden
E-mail: balb@chalmers.se

The ORCID identification number(s) for the author(s) of this article can be found under https://doi.org/10.1002/adfm.202106198.

DOI: 10.1002/adfm.202106198

on NCs is still far from satisfactory. Gray et al. used CdS/ZnS core-shell NCs as sensitizers and 2,5-diphenyloxazole (PPO) as the annihilator, achieving a TTA-UC quantum yield of 2.6%, with the emission maximum at 355 nm.[5c] Another example is a system with quantum-confined perovskite NCs as sensitizers, 1-naphthoic acid (1-NCA) as the mediator, and PPO as the annihilator, in which the TTA-UC quantum yield was reported to be 5.1%.[5d] In order to use solar energy for UV photochemistry, the challenge remains to develop visible-to-UV TTA-UC systems with significantly higher TTA-UC quantum yields, as well as producing photons of sufficiently high energy. Moreover, the systematic development of such high-performance systems requires a better understanding of the interactions between the NCs, the mediator, and the annihilator.

Herein, the various energy transfer steps influencing the TTA-UC performance are systematically investigated using three different-sized CdS NCs, four mediators, and four annihilators with different energy levels. By introducing the mediators via a direct mixing fashion, improving the quality of CdS NCs, and correlating the energy levels of CdS NCs, mediators and annihilators, we have improved the triplet energy transfer and UC efficiencies, and extended the UV light region of NC-based TTA-UC. Specifically, we demonstrate the efficiencies of triplet energy transfer from CdS NCs to the mediators are close to unity, a visible-to-UV TTA-UC quantum yields of up to 10.4% (out of a 50% maximum), and a photon energy of the UC light approaching 4 eV by alteration of the annihilator. The TTA-UC quantum yields and upconverted photon energy in our study show the best performance out of all visible-to-UV TTA-UC systems based on NCs to date, which is also close to that of the most efficient NC-based visible-to-visible TTA-UC system (12%),[9] and as high as the record efficiency and upconverted photon energy of optimized organic systems.[6e,h] More importantly, our approach provides general guidelines for the design of efficient visible-to-UV TTA-UC systems based on NCs.

Figure 1A,B shows the chemical structures and energy levels of the CdS NCs, mediators, and UV annihilators presented above. The mechanism of visible-to-UV TTA-UC based on CdS NCs is schematically shown in Figure 1C. Three groups of CdS NCs with different sizes were synthesized for sensitizing purposes. Four mediators that interact with the CdS NCs were chosen: benzoic acid (BA), biphenyl-4-carboxylic acid (4-BCA), phenanthrene-3-carboxylic acid (3-PCA), and 1-NCA. The mediators are introduced via a direct mixing fashion, which improves the efficiency of the first triplet energy transfer step (TET_1) from CdS NCs to close to unity. Four UV-emitting annihilators, namely 2,5-diphenyl-1,3,4-oxadiazole (PPD), naphthalene (Naph), *p*-terphenyl (TP), and PPO, were used to study the visible-to-UV TTA-UC performance sensitized by the CdS NCs and mediators presented above.

2. Results

2.1. Synthesis and Photophysical Characterization of CdS NCs

CdS NCs were synthesized based on literature procedures via hot-injection of elemental sulfur into a solution of cadmium fatty acid salts (see Supporting Information for synthetic details).[10] The injection and growth temperature, growth periods, and purification process were found to be crucial to form high-quality CdS NCs,[11] which featured narrow full-width of half-maximum (fwhm) emission, high photoluminescence quantum yields, and weak trap state emission. Here, three batches of CdS NCs with different sizes were synthesized by injecting the sulfur precursor at 190–230 °C and growing between 130 and 170 °C for 20–60 min. The synthesis temperature and reaction time were varied according to the required size of CdS NCs. In general, larger-sized CdS NCs were obtained by injecting and growing at a higher temperature while using a shorter reaction time. Hexane-acetonitrile precipitation were applied for the purification in accordance with previous reports, in which the impurities were quantitatively removed without degradation of the surface ligands.[12]

Figure 2 shows the UV/vis absorption and PL spectra of three batches of CdS NCs, named CdS 393, CdS 405, and CdS 426, corresponding to the first absorption peak in toluene at 393, 405, and 426 nm, respectively. The diameters of these CdS NCs were estimated from the wavelengths of the first absorption peak to be 3.1, 3.5, and 4.3 nm,[13] which were also supported by direct observation in transmission electron microscopy (TEM, Figure S1, Supporting Information). Figure 2B shows the PL spectra of three batches of CdS NCs. The typical narrow bandwidth (fwhm = 18–20 nm) emission and weak broad trap state emission at longer wavelengths were observed in all three batches, with the PL maximum at 408, 425, and 447 nm, respectively. The trap state emission with a broad peak at longer wavelength originates from the presence of sulfur vacancy sites. The relative number of sites, which acts as electron traps, is larger for the smaller CdS NCs, and the emission from these sites is, thus, expected to be stronger from CdS 393.[11c] The photophysical properties of the three batches of CdS NCs are summarized in **Table 1**.

The PL quantum yields (QY_{PL}) of these CdS NCs were determined to lie between 20% and 30%, which is significantly higher than the values previously reported (4.4%) for CdS NCs used for visible-to-UV TTA-UC.[5c] Such high QY_{PL} is the result of a longer growth period and a modified purification method. A high QY_{PL} is important because it signals that non-radiative decay channels (e.g., trap state formation) are suppressed and enables downstream TET processes to be more efficient. All three batches of CdS NCs show multi-exponential PL decays (See Figure S2 and Table S2 in the Supporting Information), which is a typical characteristic of semiconductor NCs.[14] Both amplitude-weighted, $<\tau>$, and intensity-weighted, $\hat{\tau}$, average lifetimes are listed in Table 1. The PL lifetimes of CdS NCs are in the range of tens of ns, which are too short to enable efficient TET directly to the annihilator. Therefore, a mediator with a long-lived triplet excited state is required to mediate TET from semiconductor NCs to the annihilator.[8,15]

2.2. Interactions between CdS NCs and Mediators

Previous studies on visible-to-UV TTA-UC systems based on NCs have focused mainly on only one mediator compound, 1-NCA.[5c,d,i] In order to investigate how the mediators influence the performance of TTA-UC, four mediators with different triplet (T_1) and singlet (S_1) excited state energies were chosen to

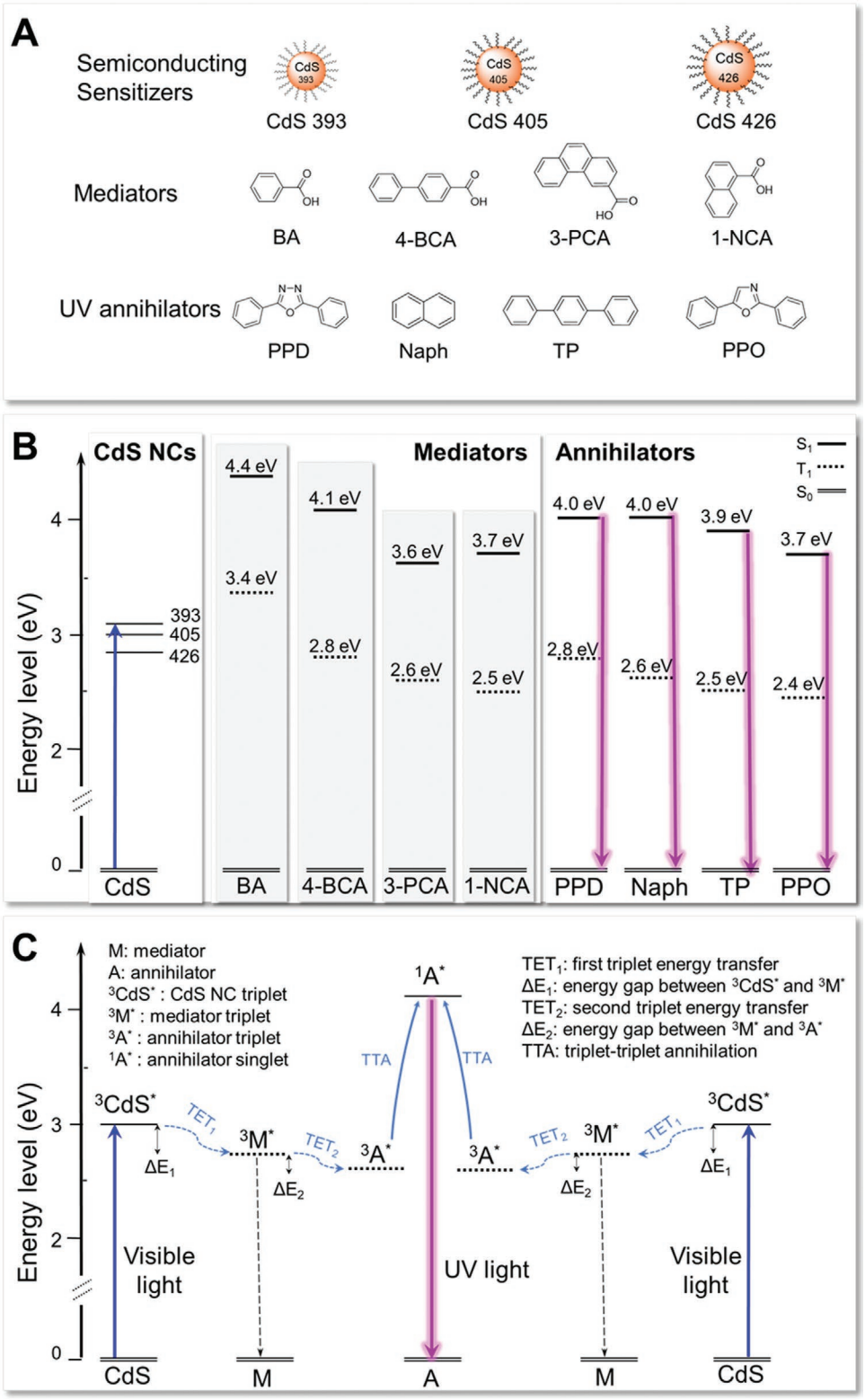

Figure 1. Chemical structures, energy levels of CdS NCs, mediators, and UV annihilators, and the mechanism of visible-to-UV photon upconversion based on CdS NCs. A) Schematic of semiconducting NCs CdS 393, CdS 405, CdS 426, chemical structures of the four mediators BA, 4-BCA, 3-PCA, and 1-NCA, and of the four UV annihilators PPD, Naph, TP, and PPO. B) Energy levels of the CdS NCs, mediators, and UV annihilators. The lowest excited singlet (S_1) and triplet (T_1) states of the mediators and annihilators are estimated from experiments and, when not available, from density functional theory calculations (see Supporting Information for calculation details and estimation of energy levels). C) The mechanism of visible-to-UV photon upconversion based on CdS NCs through two triplet energy transfer steps followed by triplet–triplet annihilation.

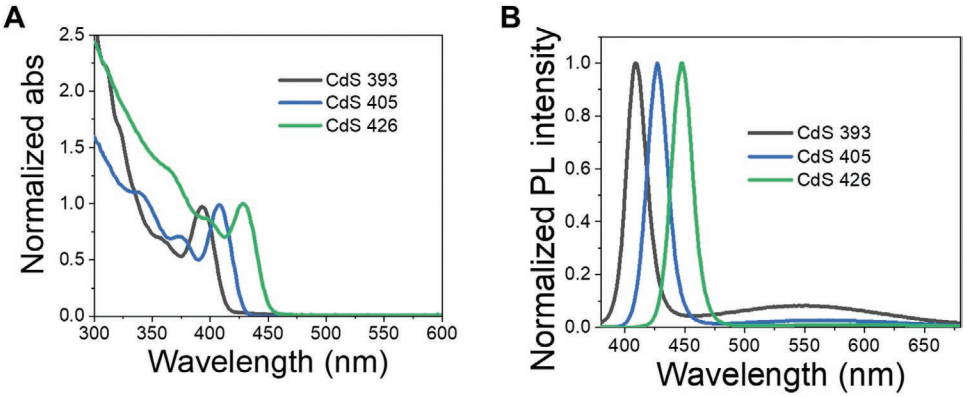

Figure 2. A) Normalized UV/vis absorption, and B) normalized PL spectra of three batches of CdS NCs in toluene.

mediate the triplet excitons from CdS NCs, see Figure 1B. The UV/vis absorption and PL spectra of these mediators are shown in Figure S3 in the Supporting Information, and their photophysical properties are summarized in **Table 2**. The carboxylic acid functional group enables the adsorption of mediators onto the surface of CdS NCs. Ligand exchange and subsequent washing steps are generally used to prepare the NC/mediator assembly. However, the low coverage of mediators on NCs after washing limits the efficiency of the TET_1 step and further TTA-UC.[16] In a previous report, where 1-NCA bound to CdS NCs was used as the sensitizer and PPO as the annihilator, the TTA-UC quantum yield was only about 0.4%.[5c] Here, in order to achieve efficient TET_1, we add excess mediators (300×10^{-6} M) into the solution of CdS NCs via a direct mixing approach, and omit any further washing steps. Directly mixing the mediators with CdS NCs can increase the number of bound ligands at equilibrium, as well as providing an excess of non-bound mediators that might function as diffusive triplet energy relays.

We first examined the PL quenching of CdS NCs upon addition of mediators. CdS 393, CdS 405, and CdS 426 solutions were prepared in toluene with the concentrations of 1.3×10^{-6}, 0.5×10^{-6}, and 0.3×10^{-6} M, respectively, yielding similar absorbances at 405 nm. The solubilities of the mediators are limited in toluene, for example, the saturation concentration of 3-PCA is about 300×10^{-6} M at room temperature. Therefore, the concentrations of the mediators were chosen to be 300×10^{-6} M for the PL quenching and following upconversion experiments. Adding BA into the CdS NCs solution did not cause any decrease of the PL intensity or the PL lifetime. The T_1 state of BA (3.4 eV) is much higher in energy than those of all three batches of CdS NCs (see Figure 1B), and TET_1 is thus thermodynamically unfavored.

The situation is different for the mediators with lower-lying T_1 states. **Figure 3** shows the PL intensity and lifetime of CdS NCs with and without the other three mediators, and Table 2 summarizes the PL lifetime and the efficiency of TET_1 (Φ_{TET1}), which was estimated from PL lifetime and intensity quenching ($\Phi_{TET1} = 1 - \langle\tau\rangle/\langle\tau\rangle_0$, where $<\boldsymbol{\tau}>$ and $<\boldsymbol{\tau}>_0$ are the amplitude-weighted average PL lifetimes of CdS NCs with and without the mediator, respectively). When 4-BCA ($E(T_1) = 2.8$ eV) is utilized as the mediator, PL quenching is only observed for the smallest NCs, i.e., CdS 393. Adding 300×10^{-6} M 4-BCA caused significant PL quenching of CdS 393 in both PL intensity and lifetime. $<\boldsymbol{\tau}>$ reduces from 16.9 ns to 5.1 ns, giving a TET_1 efficiency of 70%, which is also close to the efficiency estimated from PL intensity quenching. Adding 4-BCA into CdS 405 and CdS 426 solutions did not result in any PL quenching, indicating that the triplet energy gap between CdS NCs and the mediator (ΔE_1) should be ≥0.2 eV to allow TET_1 to occur. Adding 3-PCA or 1-NCA to the NC solutions caused a significant decrease in both PL intensity and lifetime for all three batches of CdS NCs, which is attributed to the relatively lower T_1 energies of 3-PCA (2.6 eV) and 1-NCA (2.5 eV), and results in efficient TET_1. In the cases of CdS 393 and CdS 405, 3-PCA, and 1-NCA show very high TET_1 efficiencies, with $\Phi_{TET1} \geq 90\%$. In most efficient NC-based TTA-UC systems reported previously (with TTA-UC quantum yields higher than 5%), e.g., $CsPbBr_3$ NCs, CdSe NCs, and InP NCs, the observed efficiency of TET_1 was above 80%.[5d,9,17] As shown below, the efficient TET_1 of our systems will further correlate with the high quantum yields of TTA-UC. In the case of CdS 426, which has the lowest exciton energy, the efficiency of TET_1 is reduced to 78% for 3-PCA and 58% for 1-NCA. In general, 3-PCA shows slightly higher Φ_{TET1} than 1-NCA in the solutions of CdS NCs (see Table 2), possibly due to a stronger binding affinity of 3-PCA to the surface of the CdS NCs. Alternatively, the position of the carboxylic acid group of 3-PCA might result in that the core of phenanthrene is slightly closer to the surface of NCs compared to the other mediators.

Table 1. The photophysical properties of three batches of CdS NCs in toluene.

	Abs λ_{1st}[a)] [nm]	Diameter[b)] [nm]	Lowest excited state energy[c)] [eV]	PL λ_{1st}[a)] [nm]	QY_{PL} [%]	$<\tau>$[d)] [ns]	$\hat{\tau}$[e)] [ns]
CdS 393	393	3.1	3.1	408	20.4	16.9	42.5
CdS 405	405	3.5	3.0	425	19.6	17.0	37.8
CdS 426	426	4.3	2.8	447	27.5	14.3	34.7

[a)]Measured in toluene; [b)]Calculated from the first exciton absorption peak;[13] [c)]Determined from the intersection of the normalized absorption and emission spectra; [d)]Amplitude-weighted average lifetime; [e)]Intensity-weighted average lifetime.

Table 2. Photophysical properties of the mediators and quenching characteristics of CdS NCs.

	Abs λ_{1st} [nm]	PL λ_{1st} [nm]	S_1[c] [eV]	T_1[d] [eV]	$<\tau>$[e] [ns]			Φ_{TET1}[f] [%]		
					CdS 393	CdS 405	CdS 426	CdS 393	CdS 405	CdS 426
BA	279[a]	302[a]	4.4	3.4	16.9	17.0	14.3	no[g]	no[g]	no[g]
4-BCA	269[a]	339[a]	4.1	2.8	5.11	17.0	14.3	70/80	no[g]	no[g]
3-PCA	354[b]	357[b]	3.6	2.6	1.34	1.21	3.23	92/93	93/95	78/68
1-NCA	301[b]	365[b]	3.7	2.5	1.67	1.65	5.67	90/97	90/95	58/46

[a]In ethanol; [b]In toluene; [c]Determined from the intersection of the normalized absorption and emission spectra; [d]From experiments and, when not available, from density functional theory calculations (see Supporting Information for calculation details and estimation of energy levels); [e]Amplitude-weighted average PL lifetime of CdS NCs in the presence of mediators; [f]Efficiency of TET_1 calculated from amplitude-weighted average PL lifetime quenching/steady state PL intensity quenching; [g]No triplet energy transfer is observed.

2.3. Photon Upconversion

Visible-to-UV TTA-UC sensitized by CdS NCs with selected mediators was examined using four annihilators that emit light in the UV region. PPO, which is a known UV annihilator, is applied to test the efficiency of TTA-UC. With the aim to achieve upconverted photons of high energy, three other compounds are studied, among which PPD and naphthalene without substituents (Naph) are explored as UV annihilators for the first time. The T_1 and S_1 energies are presented in Figure 1B, and the absorption and PL spectra of the annihilators are shown in Figure S4 in the Supporting Information. The QY_{PL} of the annihilators in toluene was determined to be 98% for PPD, 25% for Naph, 100% for TP, and 95% for PPO. The typical TTA-UC emission spectra of the annihilators upon 405 nm excitation in deaerated toluene are shown in **Figure 4**, which

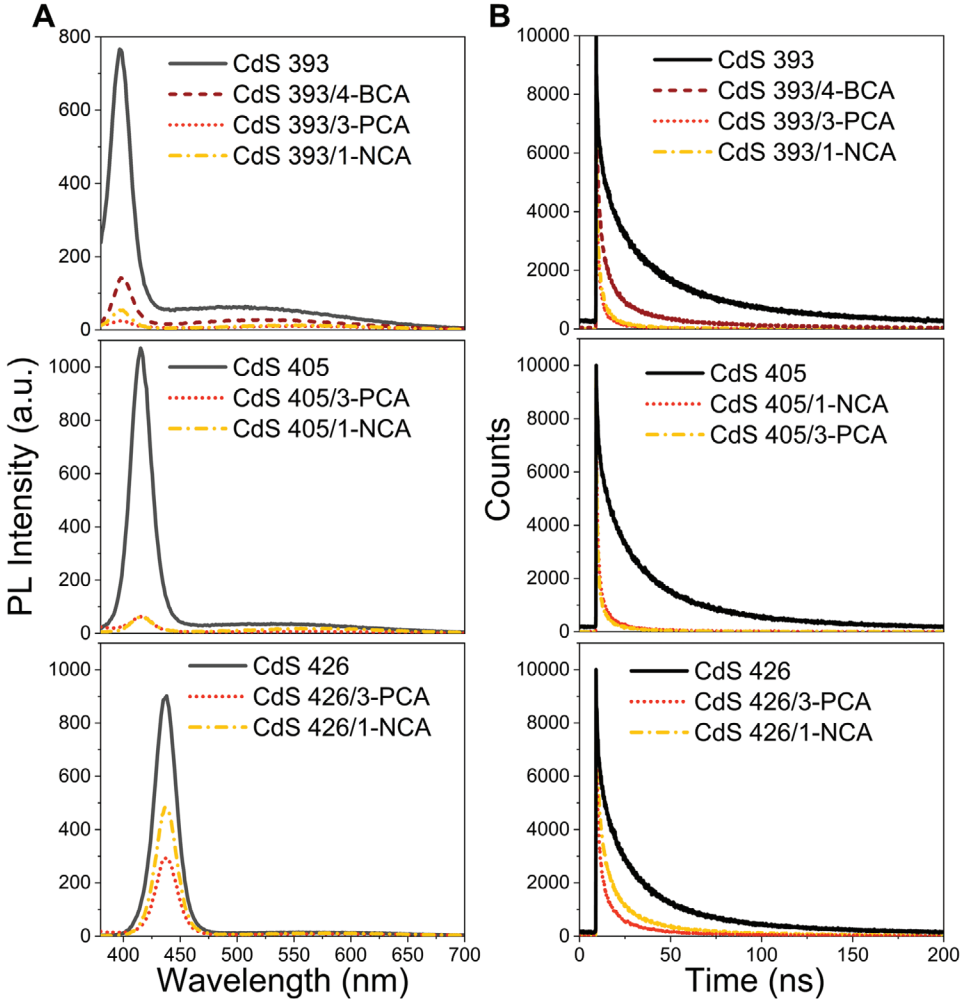

Figure 3. A) PL spectra and B) time-resolved PL decay of CdS NCs with and without the mediators 4-BCA, 3-PCA, and 1-NCA (300×10^{-6} M) in toluene.

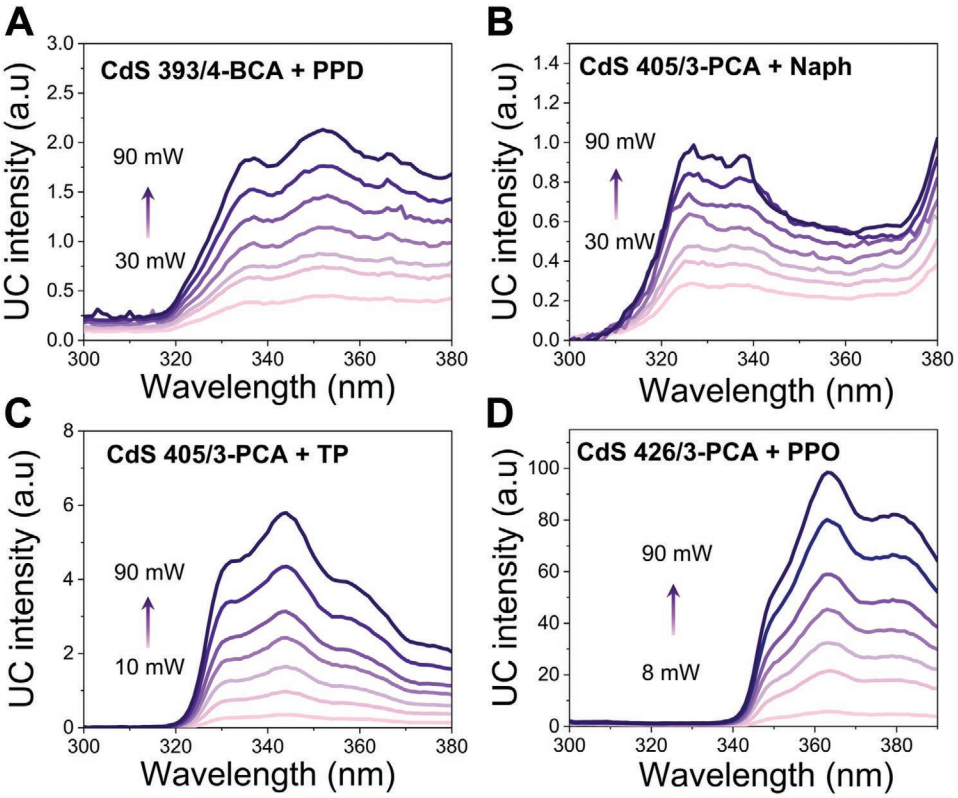

Figure 4. UC emission in deaerated toluene solution under 405 nm excitation from A) PPD (20×10^{-3} M) with CdS 393 (1.3×10^{-6} M)/4-BCA (300×10^{-6} M), and B) Naph (20×10^{-3} M) with CdS 405 (0.5×10^{-6} M)/3-PCA (300×10^{-6} M). Similar spectra were also observed using CdS 393/4-BCA, CdS 393/3-PCA, CdS 405/3-PCA, or CdS 426/3-PCA as sensitizers. C) Upconverted emission of TP (10×10^{-3} M) with CdS 405 (0.5×10^{-6} M)/3-PCA (300×10^{-6} M). Similar spectra were also observed using CdS 393/4-BCA, CdS 393/3-PCA, CdS 405/3-PCA, CdS 426/3-PCA, CdS 393/1-NCA, or CdS 405/1-NCA as sensitizers. D) Upconverted emission of PPO (5×10^{-3} M) with CdS 426 (0.3×10^{-6} M))/3-PCA (300×10^{-6} M). Similar spectra were observed in all the cases where TET_1 is allowed from the CdS NCs to the mediators. The reabsorption of UC photons by CdS NCs and mediators was alleviated by using cuvettes with a 2 mm optical path length.

cover the UV range from 310 to 400 nm. The UC emission of PPD, with the highest T_1 (2.8 eV) and S_1 (4.0 eV) energies of the four annihilators, was only observed when CdS 393/4-BCA was used as the sensitizer (Figure 4A). The T_1 energy of PPD is higher than those of 3-PCA and 1-NCA, thus, the second triplet energy transfer step (TET_2) from these mediators to PPD is not thermodynamically favored. The UC emission of Naph, with an onset at around 320 nm (Figure 4B), was observed in such instances where 4-BCA or 3-PCA were used as mediators, despite the fact that TET_2 from 3-PCA to Naph is thermodynamically slightly uphill. The energy of the upconverted photons from Naph upon 405 nm irradiation reaches as high as 3.9 eV. This is on par with the value recently reported for 1,5-naphthalenedisulfonate using organic Ir complexes as the sensitizer, which to date is the highest photon energy achieved by means of TTA-UC.[5e] No obvious UC emission from Naph is observed when using 1-NCA to mediate the triplet of CdS NCs, likely due to the lower T_1 of 1-NCA (2.5 eV) than that of Naph (2.6 eV). TP, with a T_1 energy 0.1 eV below that of Naph, also functions as an annihilator compound. In conjunction with triplet mediating 4-BCA or 3-PCA, UC emission from TP ranging from 320 to 380 nm was observed, with the first emission shoulder located at 330 nm (Figure 4C). This is very similar to the emission spectrum obtained upon direct UV light excitation (Figure S4C, Supporting Information). Unlike the case where Naph was used as the annihilator, we also observed weak UC emission from TP when using CdS 393/1-NCA or CdS 405/1-NCA as sensitizers, which can be explained by the lower-lying T_1 and higher QY_{PL} of TP. PPO has the lowest T_1 energy (2.4 eV) of all studied annihilators, and, consequently, UC emission ranging from 340 to 400 nm, with the first emission shoulder at 350 nm (Figure 4D), was observed in all cases where TET_1 from CdS NCs to the mediator is allowed. Moreover, we also observed UC emission from 5,10-dihydroindeno[2,1-a]indene (I2) (Figure S5, Supporting Information), a new annihilator that has not been reported previously. The unstructured TTA-UC emission of I2 covered approximately the same spectral range as PPO but exhibited much weaker UC intensity.

Power-dependence experiments show that the UC emission of PPO makes the expected transition from a quadratic to a linear regime when the excitation power increases (Figure S6, Supporting Information), which is a key characteristic of many TTA-UC systems.[18] The lowest excitation threshold intensity here is 0.95 W cm^{-2} for CdS 405/3-PCA, which is lower than the values of previous reports using CdS/ZnS (2.3 W cm^{-2})[5c] or perovskite NCs with 1-NCA (1.9 W cm^{-2})[5d] as sensitizers. The threshold intensity of PPD, Naph, and TP is beyond the range of our excitation source (with the maximum power of

18 W cm^{-2}), and the linear region is not observed (Figure S7, Supporting Information). Therefore, the values for the upconversion quantum yields of generated photons (Φ_{UC_g}),[19] also called the internal upconversion quantum yield, determined at 14 W cm^{-2} are evaluated in the linear excitation regime for PPO, while in an intermediate regime for PPD, Naph, and TP, leading to Φ_{UC_g} values not reaching their maxima in the latter cases.

We further determined the Φ_{UC_g} of all systems. This was done by relative actinometry (Equation (1)).

$$\Phi_{UC_g} = \Phi_r \frac{\left(1-10^{-A_r}\right)}{\left(1-10^{-A_{UC}}\right)} \frac{F_{UC}}{F_r} \frac{I_r}{I_{UC}} \frac{1}{\Phi_{out}} \quad (1)$$

Here, UC and r subscripts refer to the upconversion and reference samples, respectively. Φ_r is the PL quantum yield of the reference sample (tetracene in deaerated toluene, Φ_r = 16%),[20] A_i is the absorbance at the excitation wavelength (405 nm), F_i is the integrated emission, I_i the excitation intensity, and Φ_{out} is the output coupling yield. The maximum Φ_{UC_g} is 50% as two annihilator triplets produce one high energy photon. Φ_{UC_g} can be related to the upconversion quantum yield of observed photons (Φ_{UC}, also called the external quantum yield) and the yield of upconverted singlet excited states (Φ_{UC_s}), the relation between these quantum yields is discussed in detail in Section 5.5 of the Supporting Information. **Table 3** summarizes the Φ_{UC_g} of PPD, Naph, TP, and PPO as annihilators with different sized CdS NCs complexed with the mediators 4-BCA, 3-PCA, or 1-NCA. For PPO and TP, the external quantum yield, Φ_{UC}, is ≈9% less than Φ_{UC_g}, and for PPD and Naph Φ_{UC} is about 20% less than Φ_{UC_g}, because of the stronger reabsorption by CdS NCs and mediators in the region of 300–340 nm. In future systems a sample cuvette with shorter optical path could be used to reduce reabsorption of UC photons and improve Φ_{UC}.

The Φ_{UC_g} of PPD with CdS 393/4-BCA as the sensitizer was evaluated to be only 0.2%. The low Φ_{UC_g} is partly explained by the relatively low TET_1 efficiency from CdS 393 to 4-BCA (Φ_{TET1} = 70%). Moreover, the degenerate T_1 energies of 4-BCA and PPD (2.8 eV for both) provide only a small driving force for TET_2 from the mediator to the annihilator. Naph also shows very low Φ_{UC_g} (< 0.1%), possibly due to the low fluorescence quantum yield of Naph (four times lower than those of the other annihilators), and a rather short-lived triplet state, about one order of magnitude shorter than that of PPO.[21] Using 4-BCA as the mediator results in a slightly higher Φ_{UC_g} (0.07%) compared to 3-PCA (0.04%), possibly because of the larger driving force for TET_2 between 4-BCA and Naph (200 meV) compared to that of 3-PCA and Naph ($E(T_1) \approx 2.6$ eV for both). Φ_{UC_g} of Naph is further reduced with increasing size of the CdS NCs. It should be noted that the Φ_{UC_g} of Naph observed here is comparable to that of naphthalene derivates using organic Ir complexes as the sensitizer, which show a Φ_{UC_g} of up to ≈0.04%.[5e]

Table 3. Upconversion quantum yields of generated photons (Φ_{UC_g}, %).

Sensitizer[a)]	TET_1 allowed?	Annihilator			
		PPD	Naph	TP	PPO
CdS 393/4-BCA	Yes	0.2	0.07	1.6	2.6
CdS 393/3-PCA	Yes	–[b)]	0.04	0.4	8.8
CdS 393/1-NCA	Yes	–	–	0.2	8.4
CdS 405/4-BCA	No	–	–	–	–
CdS 405/3-PCA	Yes	–	0.03	0.2	10.4
CdS 405/1-NCA	Yes	–	–	0.1	9.1
CdS 426/4-BCA	No	–	–	–	–
CdS 426/3-PCA	Yes	–	0.01	0.08	6.0
CdS 426/1-NCA	Yes	–	–	–	3.6

[a)]Determined in deaerated toluene and excited at 405 nm (14 W cm^{-2}), with an experimental error of ≈±10%; [b)]Dash indicates that no UC emission was observed.

The Φ_{UC_g} of TP shows a very similar trend to Naph when varying the sensitizer. The highest Φ_{UC_g} of TP is observed in the presence of CdS 393/4-BCA, and Φ_{UC} is reduced when CdS 393 is paired with lower T_1 energy mediators, i.e. 3-PCA or 1-NCA. Using larger sized CdS NCs further decreased the Φ_{UC_g} of TP. However, in general, Φ_{UC_g} of TP is about 10 times higher than that of Naph using the same sensitizer. We attribute the higher Φ_{UC_g} of TP to the low-lying and longer-lived triplet state, and the higher fluorescence quantum yield.[21] PPO shows the highest Φ_{UC_g} among the four annihilators. When CdS 405/3-PCA is utilized as the sensitizer, Φ_{UC_g} of PPO reach as high as 10.4%. This is comparable with the highest visible-to-UV TTA-UC quantum yield (10.25%) achieved to date with organic molecular sensitizers.[5h] A high Φ_{UC_g} of 9.1% for PPO was also observed when mixed with CdS 405/1-NCA, which is more than 20 times higher than the value previously reported for PPO sensitized by CdS NCs with surface-anchored 1-NCA.[5c] Further increasing the size of CdS NCs to CdS 426 leads to a reduced Φ_{UC_g} of PPO, and is attributed to less efficient TET_1 from CdS 426 to 3-PCA or 1-NCA.

Upon comparison of Φ_{UC_g} for different annihilators using the same sensitizer, e.g., CdS 393/4-BCA, we found that decreasing the T_1 energy of the annihilator generally leads to an increased Φ_{UC_g}. For instance, PPD, which has the same T_1 energy as 4-BCA (2.8 eV), yields a Φ_{UC_g} of 0.2%. Meanwhile, TP and PPO, with T_1 energies ≈300 meV and 400 meV below that of 4-BCA, yield Φ_{UC} of 1.6% and 2.6%, respectively, despite having fluorescence quantum yields similar to that of PPD. When using 3-PCA or 1-NCA as the mediator, we also observed that Φ_{UC_g} increases dramatically with the increase of the energy gap between the T_1 states of the mediator and the annihilator. For example, in the case of CdS 393/3-PCA as the sensitizer, TP, with a T_1 energy similar to that of 3-PCA, shows a Φ_{UC_g} of 0.4%, while PPO, with its T_1 energy 200 meV below that of 3-PCA, gives a Φ_{UC_g} of 8.8%. This remarkable difference is likely not caused only by differences in TET efficiencies, but could also be influenced by heteromolecular TTA processes (which are discussed in more detail in the Supporting Information).

2.4. Transient Spectroscopy

To gain further insight into the mechanism of the TTA-UC process, nanosecond transient absorption (TA) and time-resolved PL spectra were measured, see **Figure 5**. Free CdS 393 shows only one transient absorption band, with a peak at 416 nm following pulsed excitation at 410 nm (black line in Figure 5A).

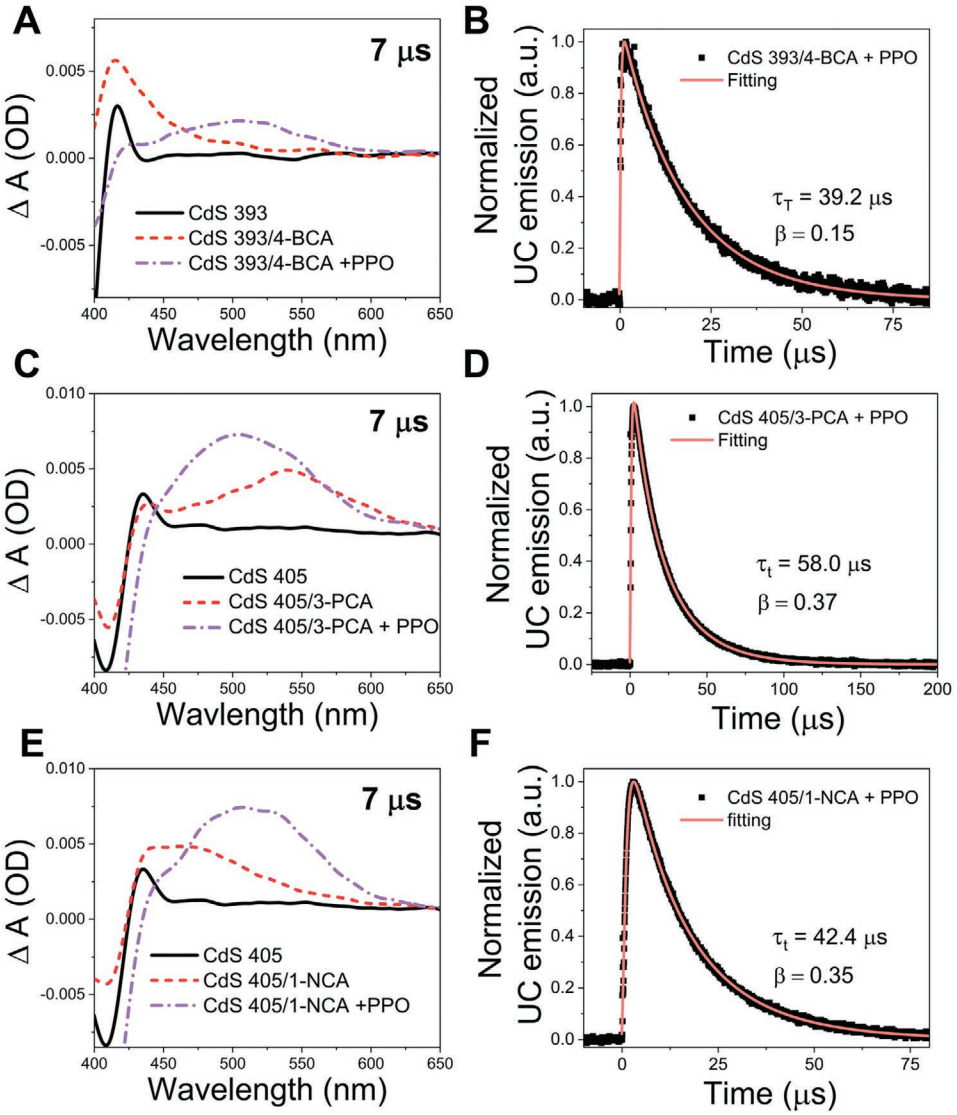

Figure 5. Nanosecond transient absorption (TA) recorded 7 μs after 410 nm pulsed excitation of CdS NCs with and without mediators and PPO, and time-resolved UC emission (TR-UC) of CdS NCs with mediators and PPO at 360 nm. A) TA of CdS 393 (black line), CdS 393/4-BCA (red dash), and CdS 393/4-BCA with PPO (purple dash-dot). B) TR-UC of CdS 393/4-BCA with PPO. C) TA of CdS 405 (black line), CdS 405/3-PCA (red dash), and CdS 405/3-PCA with PPO (purple dash-dot). D) TR-UC of CdS 405/3-PCA with PPO. E) TA of CdS 405 (black line), CdS 405/1-NCA (red dash), and CdS 405/1-NCA with PPO (purple dash-dot). F) TR-UC of CdS 405/1-NCA with PPO.

This has been attributed to the formation of the S^- radical within the CdS particles.[22] Mixing 4-BCA with CdS 393 results in an increased TA signal at 416 nm, with an additional long-lived positive feature tailing to 500 nm (red line in Figure 5A), which can be assigned to the $T_1 \rightarrow T_n$ absorption of 4-BCA, in accordance with the TA spectra of biphenyl.[23] This indicates that the T_1 state of 4-BCA is formed via TET_1 from CdS 393. The triplet lifetime of 4-BCA was determined to be 12 μs (Figure S8A,D, Supporting Information). Adding PPO into the solution of CdS 393 and 4-BCA caused a shift of the TA signal maximum from 410 to 505 nm, and a new broad TA band from 450 to 600 nm appears (purple in Figure 5A), corresponding to the $T_1 \rightarrow T_n$ absorption of PPO.[5a] This confirms the formation of the T_1 state of PPO via TET_2 from T_1 of 4-BCA. The TTA-UC emission of PPO is further confirmed by measuring the PL lifetime. Figure 5B shows the time-resolved emission decay of PPO at 360 nm in a solution of CdS 393/4-BCA upon 410 nm pulsed excitation. The measured triplet lifetime (τ_T) of PPO is 39.2 μs, which is much longer than the lifetime (<2 ns) of directly excited PPO upon UV light irradiation.[24] The fitting of the UC emission was done using Equation (2).[25]

$$I_{UC}(t) \propto \left[{}^3A^* \right]^2 = \left(\alpha_1 \exp\left(-\frac{t}{\tau_1} \right) + \alpha_2 \frac{1-\beta}{\exp\left(t/\tau_T \right) - \beta} \right)^2 \quad (2)$$

Here, $I_{UC}(t)$ is the UC emission, $[{}^3A^*]$ is the annihilator triplet concentration, t is time, τ_1 is the time constant for the rise

of emission, and α_i are preexponential factors. The dimensionless parameter β represents the relative efficiency of the TTA process and takes a value between 0 and 1, with higher values indicating more efficient TTA, see the detailed fitting and discussion in Section 5.6 of the Supporting Information. For CdS 393/4-BCA/PPO, this value is 0.15, meaning that a majority of PPO triplets decay by first-order processes.

The formation of triplet excited 3-PCA is observed upon mixing with CdS 405 (Figure 5C, red dash). A broad positive band is observed between 450 and 650 nm, and the triplet lifetime of 3-PCA is estimated to 22 µs by fitting of the TA decay at 530 nm (Figure S8E, Supporting Information). Adding PPO into the solution of CdS 405/3-PCA (purple in Figure 5C) yields a stronger PPO triplet absorption signal than that in Figure 5A, indicating a more efficient TET process overall. The triplet lifetime of PPO in the solution of CdS 405/3-PCA is 58.0 µs (fitting from Figure 5D), with a β value of 0.37. The TTA process is thus much more efficient in this system, which is expected given higher Φ_{TET1} and Φ_{UC}.

Figure 5E shows the TA spectra of CdS 405 with and without 1-NCA and PPO. Compared with bare CdS 405, adding 1-NCA yields a positive TA feature between 450 and 550 nm, corresponding to the $T_1 \rightarrow T_n$ absorption of 1-NCA.[26] By fitting the TA kinetics in Figure S8F in the Supporting Information at 450 nm, the triplet lifetime of 1-NCA is determined to be 18 µs, which is comparable to that obtained from sensitization of naphthalene triplets using $CsPbBr_3$ NCs (13.2 µs).[26] Adding PPO into the solution of CdS 405/1-NCA causes the disappearance of the 1-NCA triplet feature which is replaced with the $T_1 \rightarrow T_n$ absorption spectra of PPO, similar in shape and magnitude to that observed in Figure 5C. The triplet lifetime of PPO when mixed with CdS 405/1-NCA is 42.4 µs (Figure 5F) with a β value of 0.35, similar to the case when 3-PCA is used as the mediator. The measured τ_T of PPO (40-60 µs) agree reasonably well with that seen for other upconverting systems using PPO.[5a,i] It is reassuring that the β values obtained from fitting the UC kinetics parallels the relative Φ_{UC} from steady state measurements, as higher β values signals a higher concentration of triplet excited annihilators, leading to higher Φ_{UC}.

3. Discussions

Our investigation of CdS NC-based visible-to-UV TTA-UC reveals that the energy matching of CdS NCs, the mediator, and the annihilator is a key factor that dictates TTA-UC and governs the ability to achieve visible-to-UV TTA-UC. In particular, there are two prerequisites:

1) The first triplet excited state (T_1) of the mediator should be lower than the lowest excited state of the CdS NCs. For example, BA has a T_1 energy higher than those of all three batches of CdS NCs and, thus, no TET_1 from CdS NCs to BA is observed. When using the largest sized CdS 426, TET_1 is observed to 3-PCA (T_1 = 2.6 eV) but not to 4-BCA (T_1 = 2.8 eV). Considering that the lowest excited state of CdS 426 is ~2.8 eV, it is required that the T_1 state of the mediator lie ≈0.2 eV or more below that of the CdS NCs to achieve sufficient TET_1, which is consistent with previous studies on triplet exciton harvesting from NCs to organic molecules, and vice versa.[8b–d,31a]
2) The T_1 state of the annihilator should be equal to or lower in energy than T_1 of the mediator. For example, PPD, with a T_1 energy of 2.8 eV, shows no UC emission when paired with 3-PCA or 1-NCA. In general, a larger driving force in the TET_2 step between the mediator and the annihilator leads to stronger UC emission.

There are two major goals when developing a visible-to-UV TTA-UC system. One is to maximize the upconverted quantum yield of the system, and the other is to generate UC photons of high energy, preferably accompanied by a large apparent anti-Stokes shift. The latter is mainly dependent on the choice of annihilator. In principle, annihilators with lower T_1 and higher S_1 energies would produce larger apparent anti-Stokes shift and higher energy of the UC photons. The highest upconverted energy, approaching 4 eV, is achieved in our study when Naph is used as the annihilator, and in this case the apparent anti-Stokes shift is as large as 0.9 eV when paired with CdS 426/3-PCA. However, due to the intrinsically low PL quantum yield and short-lived triplet state of Naph, the overall Φ_{UC} is very low. Harada et al. synthesized a Naph derivative with two TIPS substituents, 1,4-bis((triisopropylsilyl)ethynyl)naphthalene, which has a PL quantum yield of 74% and a lower T_1 energy (2.1 eV), and it ends up having a high visible-to-UV quantum yield of 10.25% together with an organic Ir complex sensitizer.[5h] However, the TIPS substitution also lowers the S_1 state, resulting in a reduction of the upconverted energy, shifting the emission maximum to around 360 nm (which should be compared to 324 nm for bare Naph). The rational design of an annihilator with a lower-lying and long-lived T_1 state while keeping a high S_1 energy, combined with a near unity PL quantum yield, will be key for the development of high efficiency visible-to-UV TTA-UC systems with large apparent anti-Stokes shifts.

The upconversion quantum yields of generated photons (Φ_{UC_g}) based on NCs can be defined by Equation (3).

$$\Phi_{UC_g} = \Phi_{ISC}\Phi_{TET1}\Phi_{TET2}\Phi_{TTA}\Phi_A \quad (3)$$

Here, Φ_{ISC}, Φ_{TET1}, Φ_{TET2}, and Φ_{TTA} are the efficiencies of intersystem crossing, TET_1 from CdS NCs to the mediator, TET_2 from the mediator to the annihilator, and TTA between two annihilators, respectively, and Φ_A is the PL quantum yield of the annihilator. Φ_{TTA} and Φ_A are dependent on the intrinsic properties of the annihilator, such as nonradiative decay rates, the triplet lifetime, and higher excited state energies, in particular those of the second triplet excited state (T_2) and the first quintet excited state (Q_1). Designing new annihilators associated with high Φ_{TTA} and Φ_A in the UV light region should be one of the subjects of future studies aiming to develop high-performing TTA-UC systems.

In principle, the efficiency of TET to the annihilator is not a major concern for systems based on two organic components including only one TET step, as the concentration of the annihilator typically is high ($[A] > 1 \times 10^{-3}$ M) in solution, thus yielding a sensitization process with close to unity efficiency.[27] For three-component systems, our study reveals that Φ_{TET2} depends on the energy gap between the mediator and

the annihilator (ΔE_2), and the triplet lifetime of the mediator. In order to achieve high Φ_{TET2}, it is required: 1) a large ΔE_2 to provide a high driving force, such as in the cases with PPO, which has the lowest-lying T_1 state among all chosen annihilators; 2) a long-lived triplet state of the mediator. 3-PCA shows a relatively longer triplet lifetime compared with the other mediators in our study, and systems including 3-PCA show higher Φ_{UC} throughout, indicative of relatively efficient TET_2. Moreover, our study and other recent reports[17,28] indicate that Φ_{TET2} scales nonlinearly with changes in Φ_{TET1}.

From the sensitizers' aspect, to further improve Φ_{UC_g} of TTA-UC based on NCs, the following factors should be considered:

1) The quality of NCs. The capacity for the CdS NC to act as an energy donor is determined by their quality. High-quality NCs, which features a narrow size distribution, a narrow PL emission band, and high PL quantum yield, suffer only from minor nonradiative recombination losses, which enables efficient triplet sensitization upon light irradiation. The quality of colloidal CdS NCs can be improved by carefully controlling the feed molar ratio of Cd and sulfur sources, the reaction temperature and time, and the purification steps.[10–12] In our case, the CdS NCs were synthesized at lower temperature with a longer reaction time and purified with little impact on the quality of CdS NCs. The PL quantum yield is more than five times higher than that of previously reported CdS NCs used for visible-to-UV TTA-UC,[5c] and similar to that of other reports on high-quality CdS NCs.[10–12] Introducing microfluidics for the synthesis of NCs could also improve the reproducibility of synthesis and increase the control of the NCs' properties.[29] Moreover, it has been demonstrated that growing a few layers of an outer shell on the NCs can enhance the PL quantum yield by removing surface traps. It should be noted that the thickness of the outer shell needs to be carefully controlled, as a thicker shell can also create an energy barrier that inhibits subsequent energy transfer to surface-attached mediators.[5c,17b,30]
2) Interactions between CdS NCs and mediators. Efficient Φ_{TET1} is the key to achieve NC-based TTA-UC with high Φ_{UC_g}, which is dependent on the size of the NCs and the properties of the mediators, such as the energy difference between CdS NCs and mediators (ΔE_1), the affinity of mediators to the surface of NCs, and the influence of competing pathways on the formation of mediator triplets.[15,31] As stated previously, Φ_{TET1} correlates to the driving force for TET_1 between CdS NCs and the mediator. In general, $\Delta E_1 \geq 0.2$ eV is required from our observations, and a larger driving force provides a higher Φ_{TET1}. Previous studies demonstrated that the number of mediator molecules (m) attached to the surface of the NCs plays a crucial role in governing the energy transfer and UC efficiency, i.e., Φ_{TET1} and Φ_{UC_g} increases with higher values of m.[32] The calculation from Piland et al. indicates that $m = 16$ could achieve $\Phi_{TET1} = 0.95$.[16] However, using ligand exchange methods, it is challenging to load enough mediators onto the surface of NCs to achieve efficient Φ_{TET1} (>90%). We have observed that the PL emission of CdS NCs is heavily quenched when loading mediators via a direct mixing approach, and consequently $\Phi_{TET1} \geq 90\%$ is observed in several cases. By fitting with a Poisson distribution, the number of bound ligands using this method can be estimated to be about 20 (See Figure S9 and Table S4 in the Supporting Information). Xu et al. recently also observed that the Φ_{TET1} from CdSe NCs to oligothiophene ligand was increased via mixing with more ligands in the solution,[33] and Nienhaus et al. reported efficient visible region upconversion by mixing the mediator 9-anthracene carboxylic acid with CdSe nanoplatelets or CdTe nanorods.[34] It should be pointed out that efficient TET_1 achieved via mixing is a result of the presence of both high-affinity, surface-bound ligands, and more dynamic, weakly bound ligands, and the estimated number of bound ligands is influenced by both (see Supporting Information for a discussion on the significance of m). The solubility of the mediators is poor in toluene, causing the mediators close to the NC surface to bind via the carboxylic acid group. If further ligand exchange protocols are invoked, weakly bound mediators can easily be washed away, leaving only a few ligands bound to the NCs, which will result in lower Φ_{TET1}.

When adding an excess of the mediator, spectral overlaps and hetero-TTA between annihilator and mediator should be considered. To optimize the number of UC photons emitted from the solution, the absorptivity of the mediator should be low in the window of upconverted UV light. Alternatively, the UC sample can be prepared in a cell with an optical pass of 10–100 μm and with scattering back reflectors in a device structure. Further optimization of the concentrations of NCs and mediators to obtain high Φ_{UC_g} and low threshold intensities is one subject of our future studies. The presence of excess free mediators may operate as diffusive triplet energy relays, which could further aid the TTA process. Moreover, to avoid back Förster resonance energy transfer (FRET) from S_1 of the annihilator to S_1 of the mediator, the spectral overlap of mediator absorption and annihilator emission should be minimized, and the concentration of the mediators used should be lower than $\approx 10 \times 10^{-3}$ M (see Supporting Information for calculation details). For future practical applications, it is vitally important to obtain high external UC quantum yields under solar irradiation. Investigations on the optimized concentrations of NC-based materials using thinner optical pathlengths would allow the development of TTA-UC systems with higher external UC quantum yields and lower threshold incident powers. Alternatively, constructing practical devices which could concentrate the sunlight would also allow for more efficient harvesting of solar energy.

4. Conclusions

Visible-to-UV TTA-UC represents a potential methodology to extend the solar energy response for artificial photosynthesis and photocatalysis. Here, we have performed a comparative investigation of visible-to-UV TTA-UC based on CdS NCs by combining three different sized CdS NCs, four mediators, and four annihilators exhibiting different energy levels. High-energy TTA-UC light approaching 4 eV is observed when CdS NCs/3-PCA and Naph are used as the sensitizer and the annihilator,

respectively. A high TTA-UC quantum yield of 10.4% (out of a 50% maximum) is achieved when CdS 405/3-PCA and PPO are used as the sensitizer and annihilator, respectively. Our study does not only present a system in which facile tuning of the spectral response and high TTA-UC efficiency is controlled by the triplet energy transfer to the mediator and annihilator, but more importantly, this comprehensive investigation provides important guidelines when designing high-performance NC-based TTA-UC systems. For example, our findings indicate that the triplet level of the mediator must lie at least 200 meV below that of the NC, while the annihilator can have a triplet level similar to that of the mediator, even though a larger driving force provides higher efficiency. Moreover, high-quality NCs can facilitate the overall upconversion quantum yield, and the direct mixing approach without further washing steps for ligand exchange has proven to be an easy and efficient method to achieve high energy transfer efficiency and upconversion quantum yield. In principle, the concepts leading to the successful improvement of visible-to-UV TTA-UC can also be applied for visible-to-visible and near infrared-to-visible TTA-UC using other varieties of NCs, such as CdSe, PbS, or PbSe NCs. Ultimately, our approach will hopefully propel further development of TTA-UC systems, which may prove to be crucial components in future solar energy harvesting schemes for photovoltaics, photocatalysis, and photosynthesis.

Supporting Information

Supporting Information is available from the Wiley Online Library or from the author.

Acknowledgements

B.A. acknowledges support from the Swedish Energy Agency (contracts: 46526-1 and 36436-2).

Conflict of Interest

The authors declare no conflict of interest.

Data Availability Statement

The data that support the findings of this study are available from the corresponding author upon reasonable request.

Keywords

CdS nanocrystals, photon upconversion, semiconductor nanocrystals, triplet energy transfer, triplet–triplet annihilation

Received: July 7, 2021
Published online:

[1] a) N. J. Turro, V. Ramamurthy, J. C. Scaiano, *Photochem. Photobiol.* **2012**, *88*, 1033; b) W. M. Horspool, F. Lenci, *CRC Handbook of Organic Photochemistry and Photobiology*, 2nd ed., CRC Press, Boca Raton, FL **2004**.

[2] a) M. F. Holick, J. A. Maclaughlin, M. B. Clark, S. A. Holick, J. T. Potts, R. R. Anderson, I. H. Blank, J. A. Parrish, *Science* **1980**, *210*, 203; b) M. F. Holick, J. A. Maclaughlin, S. H. Doppelt, *Science* **1981**, *211*, 590.

[3] a) M. G. Walter, E. L. Warren, J. R. McKone, S. W. Boettcher, Q. X. Mi, E. A. Santori, N. S. Lewis, *Chem. Rev.* **2010**, *110*, 6446; b) H. Kato, K. Asakura, A. Kudo, *J. Am. Chem. Soc.* **2003**, *125*, 3082; c) C. F. Fu, X. J. Wu, J. L. Yang, *Adv. Mater.* **2018**, *30*, 1802106.

[4] a) V. Gray, D. Dzebo, M. Abrahamsson, B. Albinsson, K. Moth-Poulsen, *Phys. Chem. Chem. Phys.* **2014**, *16*, 10345; b) T. N. Singh-Rachford, F. N. Castellano, *Coord. Chem. Rev.* **2010**, *254*, 2560; c) J. Z. Zhao, S. M. Ji, H. M. Guo, *RSC Adv.* **2011**, *1*, 937; d) T. A. Lin, C. F. Perkinson, M. A. Baldo, *Adv. Mater.* **2020**, *32*, 1908175.

[5] a) T. N. Singh-Rachford, F. N. Castellano, *J. Phys. Chem. A* **2009**, *113*, 5912; b) N. Yanai, M. Kozue, S. Amemori, R. Kabe, C. Adachi, N. Kimizuka, *J. Mater. Chem. C* **2016**, *4*, 6447; c) V. Gray, P. Xia, Z. Y. Huang, E. Moses, A. Fast, D. A. Fishman, V. I. Vullev, M. Abrahamsson, K. Moth-Poulsen, M. L. Tang, *Chem. Sci.* **2017**, *8*, 5488; d) S. He, X. Luo, X. Liu, Y. L. Li, K. F. Wu, *J. Phys. Chem. Lett.* **2019**, *10*, 5036; e) B. Pfund, D. M. Steffen, M. R. Schreier, M. S. Bertrams, C. Ye, K. Borjesson, O. S. Wenger, C. Kerzig, *J. Am. Chem. Soc.* **2020**, *142*, 10468; f) W. Zhao, F. N. Castellano, *J. Phys. Chem. A* **2006**, *110*, 11440; g) P. F. Duan, N. Yanai, N. Kimizuka, *Chem. Commun.* **2014**, *50*, 13111; h) N. Harada, Y. Sasaki, M. Hosoyamada, N. Kimizuka, N. Yanai, *Angew. Chem., Int. Ed.* **2021**, *60*, 142. i) K. Okumura, N. Yanai, N. Kimizuka, *Chem. Lett.* **2019**, *48*, 1347.

[6] a) J. Peng, X. Y. Guo, X. P. Jiang, D. H. Zhao, Y. G. Ma, *Chem. Sci.* **2016**, *7*, 1233; b) Q. Chen, Y. M. Liu, X. Y. Guo, J. Peng, S. Garakyaraghi, C. M. Papa, F. N. Castellano, D. H. Zhao, Y. G. Ma, *J. Phys. Chem. A* **2018**, *122*, 6673.

[7] a) C. B. Murray, D. J. Norris, M. G. Bawendi, *J. Am. Chem. Soc.* **1993**, *115*, 8706; b) M. A. Hines, G. D. Scholes, *Adv. Mater.* **2003**, *15*, 1844; c) X. Wang, J. Zhuang, Q. Peng, Y. D. Li, *Nature* **2005**, *437*, 121.

[8] a) C. Mongin, S. Garakyaraghi, N. Razgoniaeva, M. Zamkov, F. N. Castellano, *Science* **2016**, *351*, 369; b) N. J. Thompson, M. W. B. Wilson, D. N. Congreve, P. R. Brown, J. M. Scherer, T. S. Bischof, M. F. Wu, N. Geva, M. Welborn, T. Van Voorhis, V. Bulovic, M. G. Bawendi, M. A. Baldo, *Nat. Mater.* **2014**, *13*, 1039; c) M. Tabachnyk, B. Ehrler, S. Gélinas, M. L. Böhm, B. J. Walker, K. P. Musselman, N. C. Greenham, R. H. Friend, A. Rao, *Nat. Mater.* **2014**, *13*, 1033; d) C. Mongin, P. Moroz, M. Zamkov, F. N. Castellano, *Nat. Chem.* **2018**, *10*, 225.

[9] a) A. Ronchi, C. Capitani, V. Pinchetti, G. Gariano, M. L. Zaffalon, F. Meinardi, S. Brovelli, A. Monguzzi, *Adv. Mater.* **2020**, *32*, 2002953; b) J. De Roo, Z. Y. Huang, N. J. Schuster, L. S. Hamachi, D. N. Congreve, Z. H. Xu, P. Xia, D. A. Fishman, T. Q. Lian, J. S. Owen, M. L. Tang, *Chem. Mater.* **2020**, *32*, 1461; c) Y. Han, S. He, X. Luo, Y. Li, Z. Chen, W. Kang, X. Wang, K. Wu, *J. Am. Chem. Soc.* **2019**, *141*, 13033.

[10] a) Z. Li, Y. J. Ji, R. G. Xie, S. Y. Grisham, X. G. Peng, *J. Am. Chem. Soc.* **2011**, *133*, 17248; b) J. Y. Ouyang, J. Kuijper, S. Brot, D. Kingston, X. H. Wu, D. M. Leek, M. Z. Hu, J. A. Ripmeester, K. Yu, *J. Phys. Chem. C* **2009**, *113*, 7579.

[11] a) W. W. Yu, X. G. Peng, *Angew. Chem., Int. Ed.* **2002**, *41*, 2368; b) Y. Shen, M. Y. Gee, A. B. Greytak, *Chem. Commun.* **2017**, *53*, 827; c) A. Veamatahau, B. Jiang, T. Seifert, S. Makuta, K. Latham, M. Kanehara, T. Teranishi, Y. Tachibana, *Phys. Chem. Chem. Phys.* **2015**, *17*, 2850.

[12] Y. Yang, J. Z. Li, L. Lin, X. G. Peng, *Nano Res.* **2015**, *8*, 3353.

[13] W. W. Yu, L. H. Qu, W. Z. Guo, X. G. Peng, *Chem. Mater.* **2004**, *16*, 560.

[14] a) M. G. Bawendi, P. J. Carroll, W. L. Wilson, L. E. Brus, *J. Chem. Phys.* **1992**, *96*, 946; b) P. Michler, A. Imamoglu, M. D. Mason,

P. J. Carson, G. F. Strouse, S. K. Buratto, *Nature* **2000**, *406*, 968.
[15] Z. Y. Huang, M. L. Tang, *J. Am. Chem. Soc.* **2017**, *139*, 9412.
[16] G. B. Piland, Z. Y. Huang, M. L. Tang, C. J. Bardeen, *J. Phys. Chem. C* **2016**, *120*, 5883.
[17] R. Lai, Y. Sang, Y. Zhao, K. Wu, *J. Am. Chem. Soc.* **2020**, *142*, 19825.
[18] A. Haefele, J. Blumhoff, R. S. Khnayzer, F. N. Castellano, *J. Phys. Chem. Lett.* **2012**, *3*, 299.
[19] Y. Zhou, F. N. Castellano, T. W. Schmidt, K. Hanson, *ACS Energy Lett.* **2020**, *5*, 2322.
[20] C. Burgdorff, S. Ehrhardt, H. G. Lohmannsroben, *J. Phys. Chem.* **1991**, *95*, 4246.
[21] S. L. Murov, G. L. Hug, I. Carmichael, *Handbook of Photochemistry*, 2nd ed., Marcel Dekker, New York **1993**.
[22] a) P. V. Kamat, N. M. Dimitrijevic, R. W. Fessenden, *J. Phys. Chem.* **1987**, *91*, 396; b) P. V. Kamat, T. W. Ebbsen, N. M. Dimitrijevic, A. J. Nozik, *Chem. Phys. Lett.* **1989**, *157*, 384.
[23] Y. H. Meyer, R. Astier, J. M. Leclercq, *Chem. Phys. Lett.* **1970**, *4*, 587.
[24] N. Boens, W. W. Qin, N. Basaric, J. Hofkens, M. Ameloot, J. Pouget, J. P. Lefevre, B. Valeur, E. Gratton, M. Vandeven, N. D. Silva, Y. Engelborghs, K. Willaert, A. Sillen, G. Rumbles, D. Phillips, A. J. W. G. Visser, A. van Hoek, J. R. Lakowicz, H. Malak, I. Gryczynski, A. G. Szabo, D. T. Krajcarski, N. Tamai, A. Miura, *Anal. Chem.* **2007**, *79*, 2137.
[25] S. M. Bachilo, R. B. Weisman, *J. Phys. Chem. A* **2000**, *104*, 7711.
[26] Y. Y. Han, X. Luo, R. C. Lai, Y. L. Li, G. J. Liang, K. F. Wu, *J. Phys. Chem. Lett.* **2019**, *10*, 1457.
[27] T. W. Schmidt, F. N. Castellano, *J. Phys. Chem. Lett.* **2014**, *5*, 4062.
[28] a) Z. Xu, Z. Huang, C. Li, T. Huang, F. A. Evangelista, M. L. Tang, T. Lian, *ACS Appl. Mater. Interfaces* **2020**, *12*, 36558; b) Z. Huang, Z. Xu, T. Huang, V. Gray, K. Moth-Poulsen, T. Lian, M. L. Tang, *J. Am. Chem. Soc.* **2020**, *142*, 17581.
[29] a) A. A. Volk, R. W. Epps, M. Abolhasani, *Adv. Mater.* **2020**, *32*, 2001626; b) Y. J. Song, J. Hormes, C. S. S. R. Kumar, *Small* **2008**, *4*, 698.
[30] G. L. Yang, N. Meir, D. Raanan, D. Oron, *Adv. Funct. Mater.* **2019**, *29*, 1900755.
[31] a) Z. Y. Huang, X. Li, B. D. Yip, J. M. Rubalcava, C. J. Bardeen, M. L. Tang, *Chem. Mater.* **2015**, *27*, 7503; b) M. Mahboub, H. Maghsoudiganjeh, A. M. Pham, Z. Y. Huang, M. L. Tang, *Adv. Funct. Mater.* **2016**, *26*, 6091.
[32] J. Zhang, H. Kouno, N. Yanai, D. Eguchi, T. Nakagawa, N. Kimizuka, T. Teranishi, M. Sakamoto, *ACS Photonics* **2020**, *7*, 1876.
[33] Z. H. Xu, T. Jin, Y. M. Huang, K. Mulla, F. A. Evangelista, E. Egap, T. Q. Lian, *Chem. Sci.* **2019**, *10*, 6120.
[34] a) Z. A. VanOrman, A. S. Bieber, S. Wieghold, L. Nienhaus, *Chem. Mater.* **2020**, *32*, 4734; b) Z. A. VanOrman, C. R. ContiIII, G. F. Strouse, L. Nienhaus, *Chem. Mater.* **2021**, *33*, 452.
[35] M. Wu, T.-A. Lin, J. O. Tiepelt, V. Bulović, M. A. Baldo, *Nano Lett.* **2021**, *21*, 1011.